THE JOURNAL OF PHYSICAL CHEMISTRY C

Article

pubs.acs.org/JPCC

Molecular and Electronic Structure of Self-Assembled Monolayers Containing Ruthenium(II) Complexes on Gold Surfaces

Ezequiel de la Llave, Santiago E. Herrera, Lucila P. Méndez De Leo, and Federico J. Williams*

Departamento de Química Inorgánica, Analítica y Química-Física, INQUIMAE-CONICET, Facultad Ciencias Exactas y Naturales, Universidad de Buenos Aires, Pabellón 2, Ciudad Universitaria, Buenos Aires, Argentina C1428EHA

Supporting Information

ABSTRACT: Ru(II) bipyridyl complexes were covalently bonded to self-assembled monolayers (SAM) on Au surfaces. Their molecular and electronic structure was studied by means of polarization modulation infrared reflection absorption spectroscopy (PM-IRRAS), photoelectron spectroscopies, scanning tunneling microscopy (STM) and density functional theory (DFT) calculations. We found that attaching the Ru complex to the SAM does not cause great modifications to its molecular structure, which retains the alkyl chain 30 deg tilted with respect to the surface normal. Furthermore, the Ru center is located 20 Å away from the metal surface, i.e., at a sufficient distance to prevent direct electronic interaction with the substrate. Indeed the electronic structure of the Ru complex is similar to that of the free molecule with a HOMO molecular orbital mainly based on the Ru center located 2.1 eV below the Fermi edge and the LUMO molecular orbital based on the bipyridine groups located 1 eV above the Fermi level.

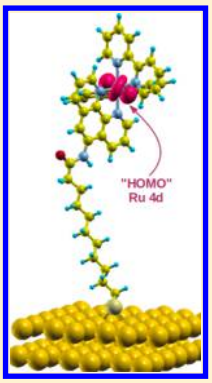

INTRODUCTION

The rising interest in the incorporation of ruthenium complexes onto ordered self-assemble arrays stems from their use as building blocks in the construction of photoactive surfaces.[1] Impelled by their applications in cell imaging,[2] immunoassays,[3] sensing,[4−6] redox active surfaces,[7] and electrogenerated chemiluminescence,[8−10] modifying electrode surfaces with ruthenium polypyridyl complexes emerges as a powerful strategy to tailor the interfacial properties of different materials in a convenient manner. The combination of both chemical stability and tunable electronic properties makes them specifically interesting in the broad field of photochemistry and photophysics.

In recent years, the binding of bis(2,2-bipyridine)-5-amino-1,10-phenanthroline ruthenium(II) (Ru(II)−NH_2) to different substrates has been presented as a valuable system with applications in biosensing and bioelectronics. Wang and co-workers[11] developed an effective electrochemiluminescence sensor combining Ru(II)−NH_2 with functionalized carbon nanotubes coated on a glassy carbon electrode. Their experimental results indicated that the modified surfaces exhibited a remarkably good detection limit for the determination of tripropylamine.[11] In a later work,[12] the Ru(II)−NH_2 complex was covalently bonded to graphite oxide constituting a sensor which displays high electrochemical activity toward the oxidation of 2-dibutylamino ethanol. This system was further applied in the determination of proline as well as the detection of methamphetamine in urine samples.[12] Finally, a simple one-pot method to synthesize luminescent Ru(II)−NH_2 functionalized gold nanoparticles with uses in sensors and bioassays was developed by Cui et al.[13]

Although the electronic structure of free Ru(II) polypyridyl complexes has been extensively studied,[14−20] it has not been studied when adsorbed on surfaces, i.e., the technologically important system. Given that the electronic properties of the adsorbed Ru complex could be influenced by the substrate and by the interaction with neighboring molecules, the study of the properties of the Ru-modified surface assembly are essential. Therefore, a clear understanding of the electronic structure of the ruthenium complex tethered on surfaces is much needed.

In this work we present a comprehensive analysis of the valence electronic structure of the Ru(II)−NH_2 complex attached to a self-assembled monolayer (SAM) over a gold surface. New insights emerge from the combination of UV photoelectron spectroscopy (UPS) and density functional theory calculations (DFT), which provide a clear description of the electronic structure of the complex tethered to the surface.

EXPERIMENTAL METHODS

Gold Substrates and Chemicals. PM-IRRAS and STM measurements were carried out using Au samples prepared as follows. Gold films (250 ± 50 nm in thickness) evaporated on a thin layer of chromium supported on glass substrates were purchased from Arrandee. Substrates were prepared by annealing for 5 min in a hydrogen flame until the film color turned to a dark red. After annealing, these polycrystalline substrates exhibit large grains with atomically smooth (111) terraces separated by steps of monatomic height. Photoelectron

Received: April 23, 2014
Revised: August 27, 2014
Published: August 28, 2014

Scheme 1. Reaction Steps Involved in the Post-Functionalization of the 11-Mercaptoundecanoic Acid SAM Au Surface with the Ruthenium Complex Monolayer

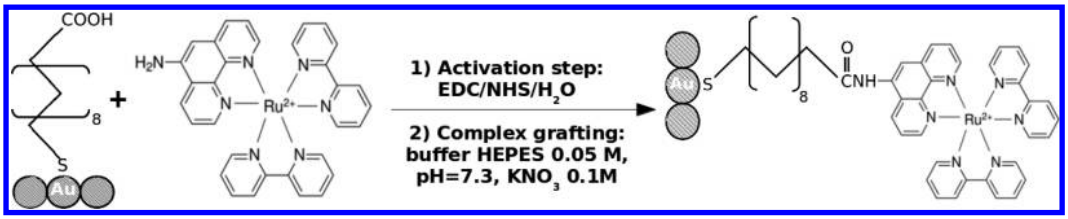

spectroscopy measurements were carried out using a polycrystalline Au sample exhibiting large (111) domains. The crystal was Ar^+ sputtered (E = 3000 eV) and annealed (T = 650 K) until no impurities are detected by XPS. Figure S1 in the Supporting Information shows the well-known herringbone reconstruction of the (111) terraces present in the Au substrates employed.

11-Mercaptoundecanoic acid (MUA), 1-ethyl-3-(3-dimethylamino-propyl) carbodiimide (EDC), *N*-hydroxysuccinimide (NHS), *N*-2-hydroxyethylpiperazine-*N*′-2-ethanesulfonic acid (HEPES), and $Ru(bpy)_2(phen\text{-}5\text{-}NH_2)(PF_6)_2$ were obtained from Sigma-Aldrich and were used as received. Absolute ethanol was of analytical grade. All solutions were prepared with 18 MΩ Milli-Q water.

Monolayer Formation. The clean gold substrates are placed in contact with a 5 mM solution of 11-mercaptoundecanoic acid in ethanol for 24 h at room temperature resulting in the formation of the 11-mercaptoundecanoic acid (MUA) SAM. Attaching the Ru complex to the MUA SAM involves postfunctionalization of the MUA SAM through a two step reaction. Scheme 1 shows the two reaction steps involved in the postfunctionalization synthetic route.[21,22] The MUA SAM is incubated for 1 h in a 40 mM EDC/10 mM NHS solution in Milli-Q water. After this first activation step, the surface is dipped overnight in 0.5 mM $Ru(bpy)_2(phen\text{-}5\text{-}NH_2)(PF_6)_2$ solution in Milli-Q water at pH ∼ 7.3 in 0.05 M HEPES buffer at an ionic strenght of 0.1 M regulated with KNO_3. Under these reaction conditions, the carboxylic terminal group exposed on the surface of the SAM readily reacts with the amine group present in the ruthenium complex forming an amide bond grafting the complex to the surface.

PM-IRRAS Measurements. Polarization modulation infrared reflection absorption spectroscopy (PM-IRRAS) experiments were performed on a Thermo Nicolet 8700 (Nicolet) spectrometer equipped with a custom-made external table-top optical mount, a MCT-A detector (Nicolet), a photoelastic modulator, PEM (PM-90 with II/Zs50 ZnSe 50 kHz optical head, Hinds Instrument), and synchronous sampling demodulator (GWC Instruments). The IR spectra were acquired with the PEM set for a half wave retardation at 2900 cm^{-1} for the CH stretching region and at 1600 cm^{-1} for C−H bending and stretching modes associated with the COOH group. The angle of incidence was set at 80°, which gives the maximum of mean square electric field strength for the air/gold interface. The demodulation technique developed by Corn[23,24] was used in this work. The signal was corrected by the PEM response using a method described by Frey et al.[25] A total of 1500 scans were performed, and the resolution was set at 4 cm^{-1}.

Photoelectron Spectroscopy Measurements. XPS measurements were performed using an ultrahigh vacuum chamber (UHV; base pressure <5 × 10^{-10} mbar) with a SPECS UHV spectrometer system equipped with 150 mm mean radius hemispherical electron energy analyzer and a nine channeltron detector. XP spectra were acquired on grounded conducting substrates at a constant pass energy of 20 eV using a Mg Kα (1253.6 eV) source operated at 12.5 kV and 20 mA at a detection angle of 30° with respect to the sample normal. Binding energies are referred to the Au $4f_{7/2}$ emission at 84 eV. UPS spectra were acquired using a He I radiation source (21.2 eV) operated at 100 mA with normal detection at a constant pass energy of 2 eV.

Scanning Tunneling Miscrocopy. STM imaging was performed in air and in constant current mode using an Agilent 5500 scanning tunneling microscope (Agilent Technologies) isolated from vibrations, air turbulence and acoustic noise. Typical tunneling currents and bias voltages were 1 nA and 0.1 V for the clean and the MUA modified Au substrate and 1 nA and 1.3 V for the Ru functionalized Au substrates. Tips were made by cutting a $Pt_{0.7}Ir_{0.3}$ 0.25 mm diameter wire with scissors at an angle of 45°. Prior their use tips were tested and calibrated imaging clean HOPG substrates obtaining atomically resolved images.

Density Functional Theory Calculations. Electronic structure calculations have been performed using density functional theory[26,27] and plane waves basis sets to expand the Kohn−Sham orbitals, as implemented in the Quantum Espresso code.[28] Ultrasoft type pseudopotentials[29] were adopted to represent the ion−electron interactions in combination with the Perdew, Burke and Ernzerhof (PBE) formalism to compute the exchange-correlation term.[30] An energy cutoff of 55 and 440 Ry was used for the plane-waves expansion of the Kohn−Sham orbitals and the charge density, respectively. k-sampling was restricted to the Γ point. The Au (111) surface was modeled as an infinite bidimensional slab, consisting of three layers of Au atoms truncated at the (111) geometry with the deepest layer of Au atoms frozen on its bulk position. The slab is separated from its periodic images in the z direction by a vacuum region of about 10 Å, enough to render the mutual interactions negligible. The calculations were performed on a supercell of size 15.05 × 17.33 × 40.13 $Å^3$, containing one adsorbate molecule.

RESULTS AND DISCUSSION

PM-IRRAS Measurements. Polarization modulated infrared reflection absorption spectroscopy (PM-IRRAS) has been employed to follow the three reaction steps, i.e. the functionalization, activation and postfunctionalization of gold substrates. Figure 1 shows the spectra of the gold surface after formation of the MUA SAM (Au/MUA), after EDC activation (Au/MUAact) and after functionalization with the Ru complex (Au/MUA/Ru). The infrared peak positions and assignments are summarized in Table 1.

All three reaction steps show peaks corresponding to the symmetric and antisymmetric stretching of CH_2 of the alkylic

dx.doi.org/10.1021/jp507199z | J. Phys. Chem. C 2014, 118, 21420−21427

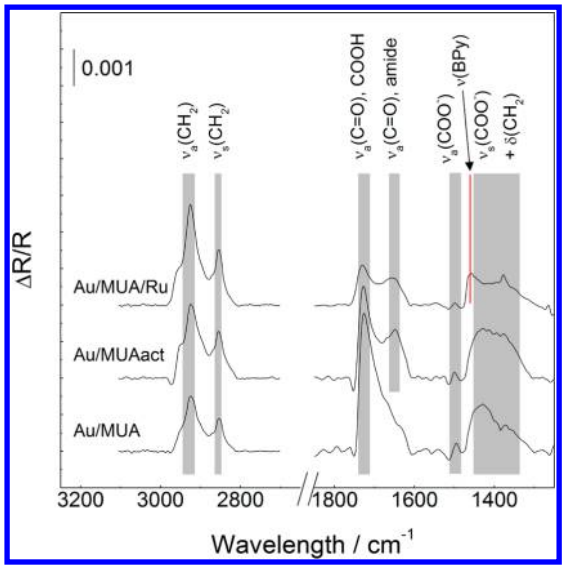

Figure 1. PMIRRA spectra of gold substrates modified by mercaptoundecanoic acid (Au/MUA), after incubation with EDC/NHS (Au/MUAact), and after postfuncitionalization with the ruthenium complex (Au/MUA/Ru).

Table 1. PMIRRAS Assignment[a]

signal assignment	Au/MUA	Au/MUAact	Au/Mua/Ru
$\nu_a(CH_2)$	2923	2923	2925
$\nu_s(CH_2)$	2854	2854	2854
ν_a(C=O) carboxylic acid	1725	1727	1730
ν_a(C=O) amide		1648	1658
$\nu_a(COO^-)$	1495	1500	1498
ν(BPy)			1456
$\delta(CH_2) + \nu_s(COO^-)$ (broad)	1430−1350	1430−1350	1430−1350

[a]All frequencies are expressed in cm^{-1}.

chains of mercaptoundecanoic acid (MUA) appearing at 2854 and around 2923 cm^{-1}. These are the typical values for this length of alkyl chain and indicate that the chains are mostly packed and in trans configuration[31] confirming formation of the dense, standing up, self-assembled monolayer. The small shift to higher wavenumbers of the antisymmetric peak for the Au/MUA/Ru sample (2925 cm^{-1}) might indicate some small degree of chain disorder after attachment of the Ru complex.

Furthermore, all three systems show the presence of the carboxylic groups confirmed by the stretching modes associated with the C═O group. In the case of Au/MUA, the peak appears at 1725 cm^{-1}, consistent with non-hydrogen-bonded (or weakly bonded) groups.[31] On the other hand, in Au/MUAact and Au/MUA/Ru, there are two peaks associated with stretching of C═O: a peak at ∼1730 cm^{-1} and another one at ∼1650 cm^{-1}. The first one is attributed to carboxylic acid that did not form an amide bond, while the second one is attributed to C═O stretching in an amide bond.[31,32] The amide bond corresponds to either the activated carbonyl (in the case of Au/MUAact) or to the carbonyl covalently bonded to the Ru complex (in the case of Au/MUA/Ru). This clearly shows that (i) the Ru complex was attached to the MUA SAM via an amide bond successfully and (ii) not all of the carboxyl acid groups in the MUA SAM reacted forming amide bonds, probably for steric reasons.

A small peak at around 1500 cm^{-1} in all three spectra can be attributed to the antisymmetric stretching of carboxylate ion, probably present in small proportions in the samples, while a broad peak at around 1440−1350 cm^{-1} can be attributed to both symmetric stretching of COO^- and CH_2 deformation modes. Finally, a small peak at 1456 cm^{-1} is observed only in the Au/MUA/Ru sample. This peak can be attributed to a stretching of the bipyridine ring coordinating the Ru ion,[22] supporting further the attachment of the Ru complex to the MUA SAM.

XPS Measurements. X-ray photoelectron spectroscopy (XPS) measurements were performed on (i) the bare Au surface, (ii) the Au substrate modified with 11-mercaptoundecanoic acid SAM (Au/MUA), and (iii) the Ru-modified monolayer (Au/MUA/Ru). Survey scans confirmed the presence of Au (in cases i, ii and iii), C, O, S (in cases ii and iii) and N and Ru (only in case iii). Figure 2 shows XP spectra for (a) Ru $3p_{3/2}$, (b) C 1s + Ru $3d_{5/2}$, (c) N 1s, and (d) Au 4f regions corresponding to the bare Au (black lines), Au/MUA SAM (red line) and Au/MUA/Ru (blue line). The absence of signals in the ruthenium, carbon and nitrogen spectra corresponding to the bare gold substrate corroborates that the initial condition prior to MUA SAM formation corresponds to a clean Au surface. Formation of the MUA SAM results in a C 1s signal consisting of two main components, one centered at 285 eV due to the C atoms in the alkane chain and a second one at 289 eV due to the carboxylic group at the end of the molecule. Finally, the Au 4f spectrum which shows the expected Au $4f_{7/2}$ (84 eV) and Au $4f_{5/2}$ (87.7 eV) doublet with a 4:3 intensity ratio is strongly attenuated by the presence of the SAM over the Au surface.

Functionalization of the MUA SAM with the Ru complex results in the presence of N and Ru on the Au surface as shown in Figure 2. The N 1s spectrum corresponding to the Ru functionalized SAM shows a signal centered around 400.5 eV which is due to the N atoms in the bipyridine and phenanthroline ring. This signal has a small shoulder at lower binding energies (around 399 eV) which is attributed to the nitrogen atoms in the amide bond.[13,33] Figure 2a shows a signal in the Ru $3p_{3/2}$ region corresponding to Ru(II) as expected. The C 1s band consists of to two mayors components: (i) the alkane chain and the pyridine rings centered around 285.9 eV and (ii) carbon bonded to more electronegative atoms centered around 288.5 eV. Note a small signal centered around 281.9 eV corresponding to the Ru $3d_{5/2}$ state in a bipyridine environment.[13] Note that, although the Ru $3d_{3/2}$ peak overlaps with the C 1s signal at 285.9 eV its contribution to the total intensity can be neglected given the low Ru complex surface coverage (see below). The measured XP spectra described above provide strong evidence supporting the formation of the Ru functionalized SAM as shown in Scheme 1. From the Ru $3d_{5/2}$ and N 1s XP signals we can calculate a Ru:N ratio of 1:9.2, this ratio is smaller than the stoichiometric ratio of 1:7 indicating that some of the EDC activated molecules did not react with the Ru complex resulting in some amide functions left at the end of the Ru functionalized SAM. Finally, a rough estimation of the Ru complex molecular coverage could be estimated from the Ru and C XP integrated intensities which gives a value of 0.4×10^{14} molecules cm^{-2}, i.e., approximately 3% of a monolayer. This estimation neglects the attenuation of the C signal and therefore it provides an overestimation of the surface coverage.

Scanning Tunneling Microscopy. Figure 3 shows STM images corresponding to the bare Au surface (A), the Au

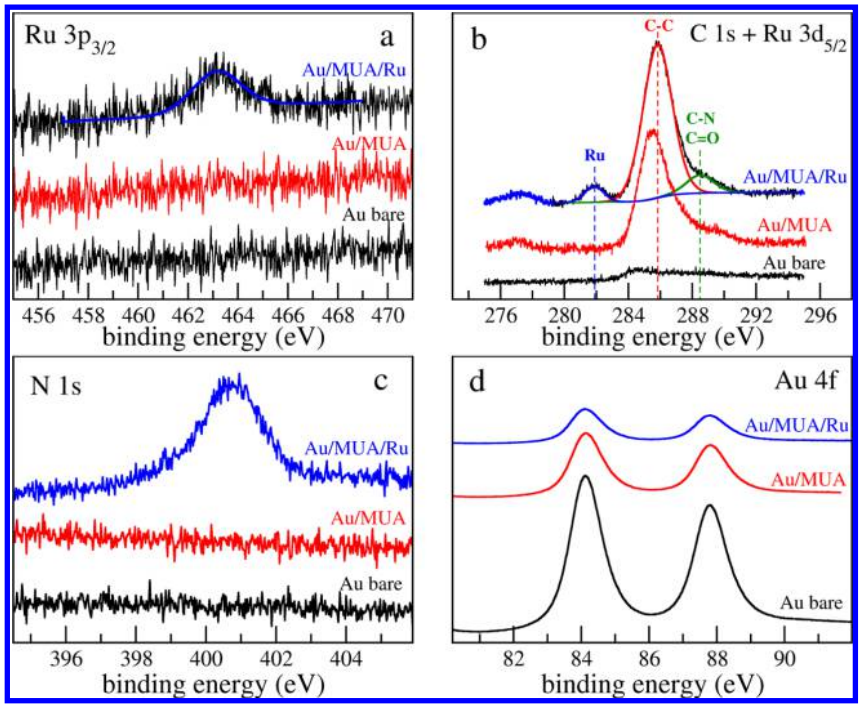

Figure 2. XPS spectra corresponding to the bare Au surface (black lines), 11-mercaptoundecanoic acid SAM (red line) and Ru complex self-assembled monolayers (blue line). (a) Ru $3p_{3/2}$, (b) C 1s + Ru $3d_{5/2}$, (c) N 1s, and (d) Au 4f regions.

substrate modified with MUA (B), and the Ru-modified monolayer (C). Large area scans of the clean Au substrate confirms that terraces are separated by steps of monatomic height. Furthermore, terraces appear homogeneous: no pits, holes or bright deposits are observed. After MUA SAM formation the picture is very different, terraces are no longer homogeneous, instead they are covered with vacancy islands (dark holes). The well-known vacancy islands formation is the result of the ejection of Au adatoms from the terraces to form thiolate–Au complexes giving further support regarding the formation of the MUA SAM over the Au substrate.[34]

Grafting the Ru complex to the MUA SAM results in the appearance of randomly distributed bright spots as observed in Figure 3C, which are assigned to the Ru complex. Note that the bright spots shown in Figure 3C present a size distribution probably due to vibration of the complex around its anchoring point. However, the important point is that bright features roughly correspond to the expected molecular size of the Ru complex. The STM Ru complex surface coverage is approximately 2% of a monolayer in agreement with the XPS overestimated value (3%).

UPS Measurements. The bottom panel of Figure 2 shows He I photoelectron spectra of the 5 eV region below the Fermi edge for (i) the bare gold substrate (black line), (ii) Au/MUA SAM (red line), (iii) Au/MUA/Ru (blue line), and (iv) Ru complex multilayers deposited over the Au substrate (bottom black line). The spectrum corresponding to the bare gold shows a very weak Fermi edge at 0 eV binding energy, a broad 6s-density of states extending from 0 eV, and a very intense 5d-density of states with the characteristics peaks at 2.7 and 4.4 eV.[35] As expected the presence of the MUA SAM completely attenuates the intensity of the Au 6s and 5d bands and does not result in any distinguishable feature in the 5 eV region below the Fermi edge. Only an increasing inelastic electron background is observed. Attaching the Ru complex to the SAM results in the appearance of a tenuous yet discernible peak at 2.9 eV below the Fermi edge. We should note that the absence of signals just below the Fermi level indicates that we can rule out direct electronic interaction with the substrate and admixing of Au 6s-states with the Ru complex LUMO.

The state at 2.9 eV below the Fermi level is better observed removing the inelastic electron background from the spectrum. The top panel of Figure 2 shows the difference between the UPS spectra of the Au/MUA/Ru and that of the Au/MUA system. Clearly the resulting spectrum shows a signal centered at 2.9 eV corresponding to a molecular electronic state of the Ru complex which could be assigned on the basis of previous measurements. Johansson et al.[18] studied the electronic structure of molecular films of $Ru(bpy)_3^{+2}$ molecules. They found that the highest occupied molecular orbital (HOMO) ruthenium metal-centered t_{2g} levels have a binding energy around 2.1 eV.[18] Therefore, the observed band at 2.9 eV below the Fermi edge could be due to photoemission from the HOMO metal-centered molecular orbital in the self-assembled monolayer. Here we should point out that the peak observed at 2.9 eV is absent in the UPS spectrum corresponding to SAMs containing only bipyridyl functional groups and also in EDC activated MUA SAMs, i.e., in the absence of the Ru complex.

Further evidence regarding the nature of the observed peak could be obtained from the spectrum corresponding to Ru complex molecular films (multilayers) deposited over the Au substrate where only the complex occupied electronic states are observed as the substrate signals are completely attenuated. This is shown in the bottom curve of Figure 4. Clearly the Ru complex has states at 2.8 and 4.4 eV below the Fermi edge which on the basis of previous[36] and our own (see below) calculations could be assigned to photoemission from a metal-centered HOMO orbital (2.8 eV) and from the ligand-centered orbital (4.4 eV) that follows in energy. Figure S2 in the Supporting Information shows the full Ru complex UPS spectrum showing the molecular electronic structure up to 10

dx.doi.org/10.1021/jp507199z | J. Phys. Chem. C 2014, 118, 21420–21427

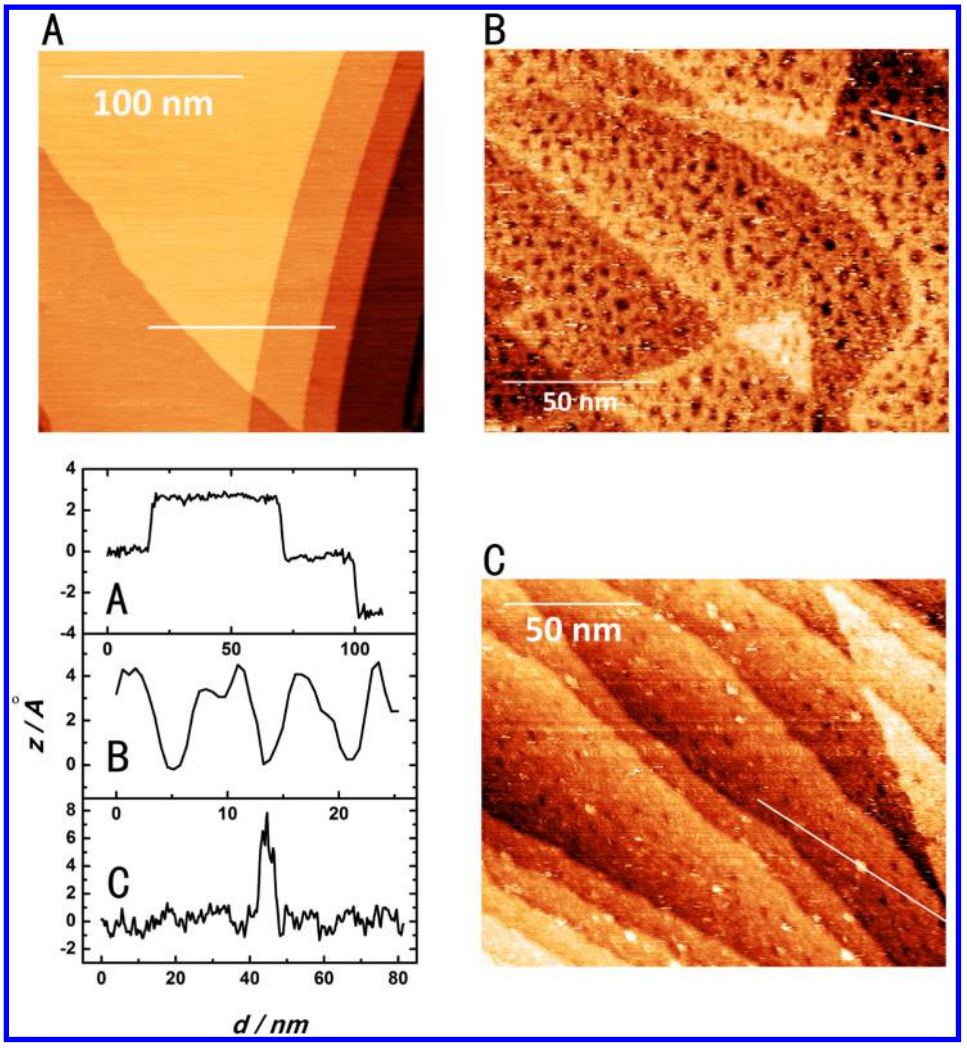

Figure 3. STM images corresponding to the bare Au surface (A), 11-mercaptoundecanoic acid SAM (B), and Ru complex self-assembled monolayers (C).

eV binding energy. The nature of these states is further explored by means of DFT calculations as follows.

DFT Calculations. The optimized geometry of the Ru complex tethered to the MUA SAM on the gold slab is shown in Figure 5. Note that the Ru complex surface coverage employed in the calculations is comparable with the molecular coverage employed in the experiments. Optimization of this model system was performed relaxing all atoms, with the exception of the inner layer of the metallic slab, which was frozen to reproduce the positions of the bulk metal. The most stable binding site, between the SAM and the gold surface, involves the coordination of the sulfur atom to a pair of Au atoms in a bridge configuration. The alkyl chain is tilted 31° with respect to the surface normal in excellent agreement with previously reported values for similar alkanethiol SAMs on Au surfaces.[37] This suggests that attaching the Ru complex does not disrupt greatly the molecular structure of the underlying SAM. The total thickness of the SAM resulting from the structure relaxation is nearly 25 Å with the Ru center approximately 20 Å away from the surface, this suggests that the Ru complex electronic structure will not be disturbed by the underlying metal as suggested by the UPS measurements discussed above. On the basis of previously published work[17] we can estimate error bars of 2 degrees in the angles and 0.05 Å in the distances.

The electronic structure of the Ru-functionalized SAM can be calculated from the projected density of states (PDOS) in the region near to the Fermi edge. In a molecule, the total density of states is the molecular orbital diagram and the corresponding PDOS will show the contribution of selected atomic orbitals to the molecular orbitals. Similarly, in an extended system the PDOS reflects the contribution of a particular atomic orbital to the overall density of states.

Figure 6 depicts the PDOS corresponding to the Ru 4d, C 2p, and N 2p states of the ruthenium complex present in the SAM. A sharp peak 2.1 eV below the Fermi level originating in the 4d electrons of the ruthenium atom (black line) with a small contribution from the 2p states of the pyridine carbons (orange line) is observed. This state corresponds to the HOMO molecular orbital of the Ru complex SAM. The position of this band is shifted nearly 0.8 eV with respect to the band observed in the UPS spectrum in Figure 4 at 2.9 eV. Such a shift was observed by us[38] and others[18] in the past and may be ascribed to the limitations in modeling neglecting final state effects and interactions with the counterions. In any case, our DFT calculations suggest that the experimentally observed state corresponds to the HOMO molecular orbital of the Ru

dx.doi.org/10.1021/jp507199z | J. Phys. Chem. C 2014, 118, 21420−21427

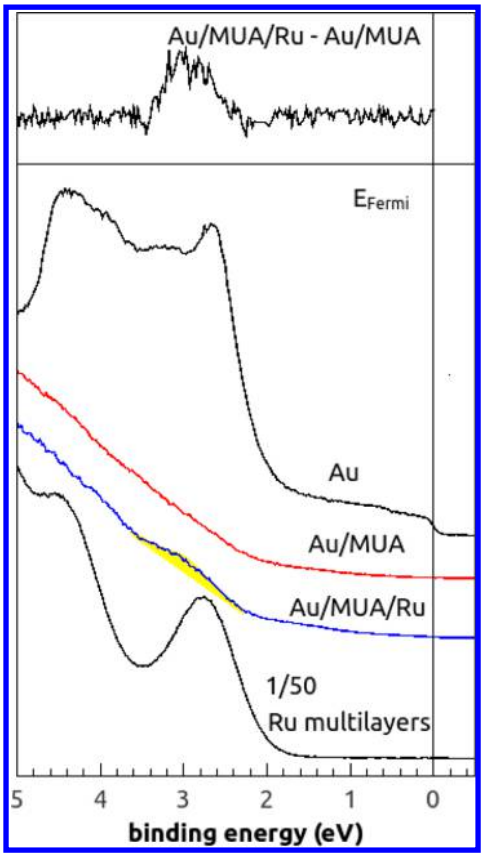

Figure 4. Bottom panel: UPS spectra of the bare gold substrate (Au bare), 11-mercapto-undecanoic acid SAM (Au/MUA), Ru complex containing SAM (Au/MUA/Ru) and Ru complex multilayers showing the density of states in the region below the Fermi level. Top panel: Difference spectrum between the Ru complex SAM and 11-mercaptoundecanoic acid SAM.

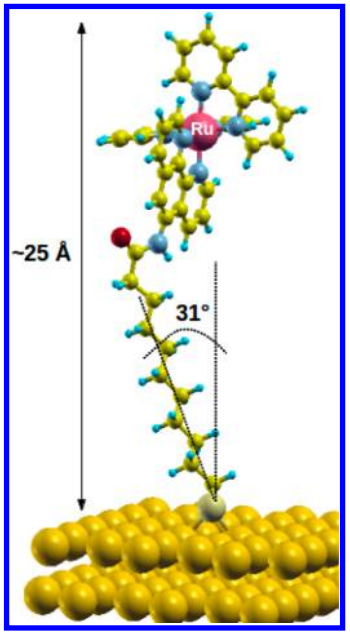

Figure 5. Molecular structure of the bis(2,2 -bipyridine)-5-amino-1,10-phenanthroline ruthenium(II) (Ru(II)−NH_2) tethered to a 11-mercaptoundecanoic acid SAM over a gold surface, as obtained from DFT geometry relaxation under periodic boundary conditions.

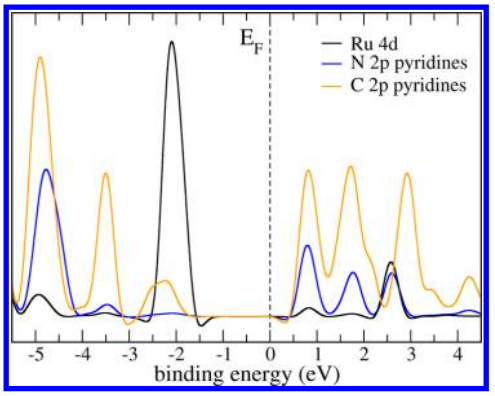

Figure 6. Projected density of states around the Fermi level for Ru 4d, C 2p and N 2p states computed from the Ru-functionalized SAM DFT calculations.

complex with major contributions of the Ru 4d state and minor contributions of the C 2p electrons. Furthermore, the following occupied molecular orbital is a ligand-centered orbital approximately 1.4 eV lower in energy. This is in excellent agreement with the UPS results discussed above where the top occupied orbitals corresponding to the Ru complex multilayers where located at 2.8 eV (HOMO) and 4.4 eV from the Fermi edge.

Figure 6 also shows that the lowest unoccupied molecular orbital (LUMO) orbital of the complex, 1 eV above the Fermi level, has a major contribution from carbon and nitrogen pyridine atoms, and a marginal contribution from the metal center *d* states. Both HOMO and LUMO orbitals of the ruthenium complex are better visualized in the isosurfaces shown in Figure 7. As discussed above, the HOMO is mainly based on the metal center, while the LUMO is mainly based on the bipyridine groups.

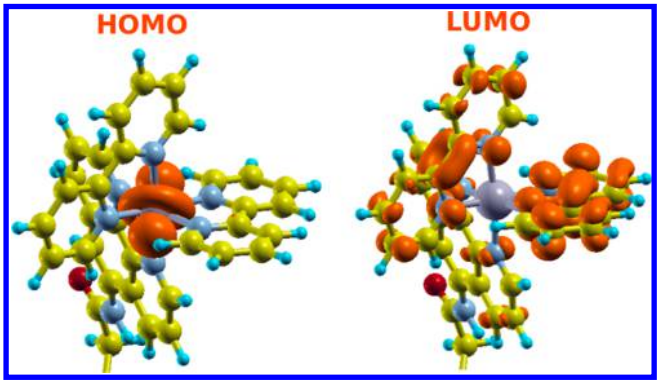

Figure 7. HOMO and LUMO of the Ru complex. Orange isosurfaces drawn at 0.002 e $bohr^{-3}$ are superimposed on the complex structure. For image clarity, only the complex is shown.

The results discussed above are in close agreement with previous reported calculations for other ruthenium polypyridine complexes.[18] Moreover, they are in line with the fact that this type of compounds have UV−vis absoption spectra dominated by metal-to-ligand charge transfer transitions.[17] Finally, our DFT calculations indicate that there is no direct electronic interaction between the Ru complex and the Au surface in agreement with the observed UPS spectrum.

dx.doi.org/10.1021/jp507199z | J. Phys. Chem. C 2014, 118, 21420−21427

CONCLUSIONS

The molecular and electronic structure of self-assembled monolayers modified with Ru(II) bipyridyl complexes on Au surfaces was studied by means of photoelectron spectroscopies, PM-IRRAS, STM, and density function theory calculations. We found that the Ru(II) complex is covalently bonded via an amide bond to the alkyl chain which is tilted 30 deg with respect to the surface normal. Furthermore, the Ru metal center is 20 Å away from the Au topmost layer and the binding site between the SAM and the gold surface involves the coordination of the sulfur atom to a pair of Au atoms in a bridge configuration. Moreover, the metal surface does not disrupt the electronic structure of the Ru complex. Indeed the HOMO orbital is mainly Ru based and is located around 2.9 eV below the Fermi level, whereas the LUMO orbital is mainly bipyridine based and is located 1 eV above the Fermi level. Therefore, our findings provide a clear description of the electronic structure of the Ru complex tethered to a Au surface which represents an important subject in the fields of photoactive surfaces and sensors.

ASSOCIATED CONTENT

Supporting Information

AFM phase image of the Au(111) surface, He I UPS spectra of Ru bipyridyl complex molecular films, and complete ref 28. This material is available free of charge via the Internet at http://pubs.acs.org.

AUTHOR INFORMATION

Corresponding Author

*(F.J.W.) E-mail: fwilliams@qi.fcen.uba.ar. Telephone: +54 11 45763380 ext 105.

Notes

The authors declare no competing financial interest.

ACKNOWLEDGMENTS

Funding from CONICET and AGENCIA is gratefully acknowledged. We acknowledge time allocation for all the DFT calculations in the supercomputer *Cristina* funded by ANPCYT.

REFERENCES

(1) Forster, R. J.; Keyes, T. E. Photonic Interfacial Supramolecular Assemblies Incorporating Transition Metals. *Coord. Chem. Rev.* **2009**, *253*, 1833−1853.

(2) Rogers, N. J.; Claire, S.; Harris, R. M.; Farabi, S.; Zikeli, G.; Styles, I. B.; Hodges, N. J.; Pikramenou, Z. High Coating of Ru(II) Complexes on Gold Nanoparticles for Single Particle Luminescence Imaging in Cells. *Chem. Commun.* **2014**, *50*, 617−619.

(3) Kurita, R.; Arai, K.; Nakamoto, K.; Kato, D.; Niwa, O. Development of Electrogenerated Chemiluminescence-Based Enzyme Linked Immunosorbent Assay for Sub-pM Detection. *Anal. Chem.* **2010**, *82*, 1692−1697.

(4) Chu, B.W.-K.; Yam, V.W.-W. Sensitive Single-Layered Oxygen-Sensing Systems: Polypyridyl Ruthenium(II) Complexes Covalently Attached or Deposited as Langmuir−Blodgett Monolayer on Glass Surfaces. *Langmuir* **2006**, *22*, 7437. 10.

(5) Li, S.; Zhong, X.; Yang, H.; Hu, Y.; Zhang, F.; Niu, Z.; Hu, W.; Dong, Z.; Jin, J.; Li, R.; Ma, J. Noncovalent Modified Graphene Sheets with Ruthenium(II) Complexes Used as Electrochemiluminescent Materials and Photosensors. *Carbon* **2011**, *49*, 4239−4245.

(6) Yu, Y.; Zhou, M.; Shen, W.; Zhang, H.; Cao, Q.; Cui, H. Synthesis of Electrochemiluminescent Graphene Oxide Functionalized with a Ruthenium(II) Complex and its Use in the Detection of Tripropylamine. *Carbon* **2012**, *50*, 2539−2545.

(7) Eckermann, A. M.; Feld, D. J.; Shaw, J. A.; Meade, T. J. Electrochemistry of Redox-Active Self-Assembled Monolayers. *Coord. Chem. Rev.* **2010**, *254*, 1769−1802.

(8) Bertoncello, P.; Kefalas, E. T.; Pikramenou, Z.; Unwin, P. R.; Forster, R. J. Adsorption Dynamics and Electrochemical and Photophysical Properties of Thiolated Ruthenium 2,2′-Bipyridine Monolayers. *J. Phys. Chem. B* **2006**, *110*, 10063−10069.

(9) Dennany, L.; O'Reilly, E.; Forster, R. J. Electrochemiluminescent Monolayers on Metal Oxide Electrodes: Detection of Amino Acids. *Electrochem. Commun.* **2006**, *8*, 1588−1594.

(10) Yuan, Y.; Li, H.; Han, S.; Hu, L.; Parveen, S.; Cai, H.; Xu, G. Immobilization of Tris(1,10-phenanthroline)Ruthenium with Graphene Oxide for Electrochemiluminescent Analysis. *Anal. Chim. Acta* **2012**, *720*, 38−42.

(11) Tao, Y.; Lin, Z.-J.; Chen, X.-M.; Huang, X.-L.; Oyama, M.; Chen, X.; Wang, X.-R. Functionalized Multiwall Carbon Nanotubes Combined with Bis(2,2 -bipyridine)-5-amino-1,10-phenanthroline Ruthenium(II) as an Electrochemiluminescence Sensor. *Sens. Actuators, B* **2008**, *129*, 758−763.

(12) Chen, X.-M.; Wu, G.-H.; Chen, J.-M.; Jiang, Y.-Q.; Chen, G.-N.; Oyama, M.; Chen, X.; Wang, X.-R. A Novel Electrochemiluminescence Sensor Based on Bis(2,2 -bipyridine)-5-amino-1,10-phenanthroline Ruthenium(II) Covalently Combined with Graphite Oxide. *Biosens. Bioelectron.* **2010**, *26*, 872−876.

(13) Yu, Y.; Zhoub, M.; Cui, H. Synthesis and Electrochemiluminescence of Bis(2,20-bipyridine)(5-amino-1,10-phenanthroline) Ruthenium(II)-Functionalized Gold Nanoparticles. *J. Mater. Chem.* **2011**, *21*, 12622−12625.

(14) Nazeeruddin, M. K.; De Angelis, F.; Fantacci, S.; Selloni, A.; Viscardi, G.; Liska, P.; Ito, S.; Takeru, B.; Gratzel, M. Combined Experimental and DFT-TDDFT Computational Study of Photoelectrochemical Cell Ruthenium Sensitizers. *J. Am. Chem. Soc.* **2005**, *127*, 16835−16847.

(15) De Angelis, F.; Fantacci, S.; Selloni, A.; Nazeeruddin, M. K.; Gratzel, M. Time-Dependent Density Functional Theory Investigations on the Excited States of Ru(II)-Dye-Sensitized TiO_2 Nanoparticles: The Role of Sensitizer Protonation. *J. Am. Chem. Soc.* **2007**, *129*, 14156−14157.

(16) Srnec, M.; Chalupsky, J.; Fojta, M.; Zendlova, L.; Havran, L.; Hocek, M.; Kyvala, M.; Rulisek, L. Effect of Spin−Orbit Coupling on Reduction Potentials of Octahedral Ruthenium(II/III) and Osmium(II/III) Complexes. *J. Am. Chem. Soc.* **2008**, *130*, 10947−10954.

(17) Abrahamsson, M.; Jager, M.; Kumar, R. J.; Osterman, T.; Persson, P.; Becker, H. C.; Johansson, O.; Hammarstrom, L. Bistridentate Ruthenium(II)polypyridyl-Type Complexes with Microsecond 3MLCT State Lifetimes: Sensitizers for Rod-Like Molecular Arrays. *J. Am. Chem. Soc.* **2008**, *130*, 15533−15542.

(18) Johansson, E. M. J.; Odelius, M.; Plogmaker, S.; Gorgoi, M.; Svensson, S.; Siegbahn, H.; Rensmo, H. Spin-Orbit Coupling and Metal-Ligand Interactions in Fe(II), Ru(II), and Os(II) Complexes. *J. Phys. Chem. C* **2010**, *114*, 10314−10322.

(19) Gorelsky, S. I.; Dodsworth, E. S.; Lever, A. B. P.; Vlcek, A. A. Trends in Metal−Ligand Orbital Mixing in Generic Series of Ruthenium N-donor Ligand Complexes—Effect on Electronic Spectra and Redox Properties. *Coord. Chem. Rev.* **1998**, *174*, 469−494.

(20) Vlcek, A.; Zalis, S. Modeling of Charge-Transfer Transitions and Excited States in d6 Transition Metal Complexes by DFT Techniques. *Coord. Chem. Rev.* **2007**, *251*, 258−287.

(21) Sehgal, D.; Vijay, K. A Method for the High Efficiency of Water-Soluble Carbodiimide-Mediated Amidation. *Anal. Biochem.* **1994**, *218*, 87−91.

(22) Ricci, A. M.; Tognalli, N.; de la Llave, E.; Vericat, C.; Mendez De Leo, L. P.; Williams, F. J.; Scherlis, D.; Salvarezza, R.; Calvo, E. J. Electrochemistry of $Os(2,2'bpy)_2Cl\ PyCH_2NHCOPh$ Tethered to Au Electrodes by S−Au and C−Au Junctions. *Phys. Chem. Chem. Phys.* **2011**, *13*, 5336−5345.

(23) Barner, B. J.; Green, M. J.; Saez, E. I.; Corn, R. M. Polarization Modulation Fourier Transform Infrared Reflectance Measurements of Thin Films and Monolayers at Metal Surfaces Utilizing Real-Time Sampling Electronics. *Anal. Chem.* **1991**, *63*, 55−60.
(24) Green, M. J.; Barner, B. J.; Corn, R. M. Real-Time Sampling Electronics for Double Modulation Experiments with Fourier Transform Infrared Spectrometers. *Rev. Sci. Instrum.* **1991**, *62*, 1426−1430.
(25) Frey, B. L.; Corn, R. M.; Weibel, S. C. *Polarization-Modulation Approaches to Reflection-Absorption Spectroscopy*; John Wiley & Sons: New York, 2001; Vol. 2, p 1042−1056.
(26) Hohenberg, P.; Kohn, W. Inhomogeneous Electron Gas. *Phys. Rev.* **1964**, *136*, B864−B871.
(27) Kohn, W.; Sham, L. J. Self-Consistent Equations Including Exchange and Correlation Effects. *Phys. Rev.* **1965**, *140*, A1133−A1138.
(28) Giannozzi, P.; Baroni1, S.; Bonini, N.; Calandra, M.; Car, R.; Cavazzoni, C.; Ceresoli, D.; Chiarotti, G. L.; Cococcioni, M.; Dabo, I.; et al. QUANTUM ESPRESSO: A Modular and Open-Source Software Project for Quantum Simulations of Materials. *J. Phys.: Condens. Matter* **2009**, *21*, 395502.
(29) Vanderbilt, D. Soft Self-Consistent Pseudopotentials in a Generalized Eigenvalue Formalism. *Phys. Rev. B* **1990**, *41*, 7892−7895.
(30) Perdew, J. P.; Burke, K.; Ernzerhof, M. Generalized Gradient Approximation Made Simple. *Phys. Rev. Lett.* **1996**, *77*, 3865−3868.
(31) Nuzzo, R. G.; Dubois, L. H.; Allara, D. L. Fundamental Studies of Microscopic Wetting on Organic Surfaces. 1. Formation and Structural Characterization of a Self-Consistent Series of Polyfunctional Organic Monolayers. *J. Am. Chem. Soc.* **1990**, *112*, 558−569.
(32) Lin-Vein, D.; Colthup, N. B.; Fateley, W. B..and Grasselli, J. G. *The Handbook of Infrared and Raman Characteristic Frequencies of Organic Molecules*; Academic Press Inc.: San Diego, CA, 1991.
(33) de la Llave, E.; Clarence, R.; Schiffrin, D. J.; Williams, F. J. Organization of Alkane Amines on a Gold Surface: Structure, Surface Dipole, and Electron Transfer. *J. Phys. Chem. C* **2014**, *118*, 468−475.
(34) Vericat, C.; Vela, M. E.; Benitez, G.; Carro, P.; Salvarezza, R. C. Self-Assembled Monolayers of Thiols and Dithiols on Gold: New Challenges for a Well-Known System. *Chem. Soc. Rev.* **2010**, *39*, 1−30.
(35) Alloway, D. M.; Hofmann, M.; Smith, D. L.; Gruhn, N. E.; Graham, A. L.; Colorado, R.; Wysocki, V. H.; Lee, T. R.; Lee, P. A.; Armstrong, N. R. Interface Dipoles Arising from Self-Assembled Monolayers on Gold: UV−Photoemission Studies of Alkanethiols and Partially Fluorinated Alkanethiols. *J. Phys. Chem. B* **2003**, *107*, 11690−11699.
(36) Westermark, K.; Rensmo, H.; Lees, A. C.; Vos, J. G.; Siegbahn, H. Electron Spectroscopic Studies of Bis-(2,2-bipyridine)(4,4-dicarboxy-2,2-bipyridine)ruthenium(II) and Bis-(2,2-bipyridine)(4,4-dicarboxy-2,2-bipyridine)osmium(II) Adsorbed on Nanostructured TiO_2 and ZnO Surfaces. *J. Phys. Chem. B* **2002**, *106*, 10108−1011.
(37) Vericat, C.; Vela, M. E.; Benitez, G. A.; Gago, J. A. M.; Torrelles, X.; Salvarezza, R. C. Surface Characterization of Sulfur and Alkanethiol Self-Assembled Monolayers on Au(111). *J. Phys.: Condens. Matter* **2006**, *18*, R867−900.
(38) Méndez De Leo, L. P.; de la Llave, E.; Scherlis, D.; Williams, F. J. Molecular and Electronic Structure of Electroactive Self-Assembled Monolayers. *J. Chem. Phys.* **2013**, *138*, 114707.